

Received May 26, 2019, accepted July 9, 2019, date of publication July 17, 2019, date of current version July 30, 2019.

Digital Object Identifier 10.1109/ACCESS.2019.2928869

# Characteristics of Tin Oxide Chromatographic Detector for Dissolved Gases Analysis of Transformer Oil

JINGMIN FAN<sup>1</sup>, (Member, IEEE), ZHE LIU<sup>1</sup>, ANBO MENG<sup>1</sup>, HAO YIN<sup>1</sup>,  
QIUQIN SUN<sup>2</sup>, FENG BIN<sup>2</sup>, AND QINJI JIANG<sup>3</sup>

<sup>1</sup>School of Automation, Guangdong University of Technology, Guangzhou 510012, China

<sup>2</sup>College of Electrical and Information Engineering, Hunan University, Changsha 410082, China

<sup>3</sup>State Grid Hunan Maintenance Company, Changsha 41007, China

Corresponding author: Qiuqin Sun (sunqq@hnu.edu.cn)

This work was supported by the National Natural Science Foundation of China under Grant 61876040 and Grant 51677061.

**ABSTRACT** The analysis of dissolved gases in insulation oil is of great significance to transformer status evaluation. In this paper, a chromatographic detector based on the nano-tin oxide fiber as well as a chromatography system is developed. The mechanism of the sensor for detecting six component feature gases (i.e., H<sub>2</sub>, CO, CH<sub>4</sub>, C<sub>2</sub>H<sub>4</sub>, C<sub>2</sub>H<sub>6</sub>, and C<sub>2</sub>H<sub>2</sub>) in transformer oil is expounded, on basis of which the exponent-logarithmic model between conductance and gas concentrations is proposed. Then, the repeatability and accuracy of the nano-tin oxide detectors are tested. The experimental results show that the gases mixture can be separated well by the designed gas chromatography system, and six component gases mixture detection can be realized by the developed detector. Meanwhile, by using the proposed model, high precision of dissolved gas measurement can be achieved, thus the validity of the presented model is verified. Moreover, compared with other chromatographic detectors, i.e., flame ionization detector, the only carrier gas needed for the nano-tin oxide chromatographic detector is the synthetic air, the hardware cost and complexity of system are reduced largely, showing promising applicable value in the engineering practice.

**INDEX TERMS** Power transformer, chromatography, dissolved gas analysis, nano-tin oxide detector.

## I. INTRODUCTION

In the past decades, with the construction of intelligent power grid [1], as well as the digitalization and informatization of substations [2], [3], the periodical maintenance of power transformer will be replaced by the condition based maintenance gradually [4], [5]. To achieve this, it is the basis that the data of the power transformer status is collected [6], [7]. Dissolved gas analysis (DGA) of transformer oil is one of the most important methods to detect the latent fault of oil-immersed power transformers [8]. It is worth mentioned that the accuracy and stability of the measuring instrument are affected by gas sensors greatly [9]–[12].

Nowadays, the on-line monitoring devices of DGA based on various gas sensors [13]–[17] have been widely used in the field of transformer status evaluation. Researchers around the world have made a lot of progresses in the development of gas sensors for on-line DGA monitoring. However, there also

exist many defects, such as the SOFC detector [17], [18] has high sensitivity but limited detection range, thermal conductivity sensor [19] are responsive to all gases, but the sensitivity is low, and high-cost helium is needed to be carrier gas. Flame ionization detector (FID) [20], has both high sensitivity and relative wide detection range, but three types of carrier gases are needed, including hydrogen which is not allowed to be used in substation. Moreover, too many carrier gases lead to complex pipeline system. The photoacoustic spectroscopy sensor (PSS) [6], [9] does not need any carrier gas, nor does the separation of mixed gas, but the sensitivity is low, and the interference of electromagnetic noises is heavy. Meanwhile, the cost of PSS is high.

In order to monitor the status of the oil-immersed power transformers more efficiently and economically, the defects of these gas sensors, i.e., the measuring accuracy, cross sensitivity, long-term stability, and high cost of gas sensors should be improved. Hence, new types of gas sensors are needed to be designed. Recently, with the development of non-material technology [21], sensors developed by nanometer

The associate editor coordinating the review of this manuscript and approving it for publication was Hui Ma.

semiconductor materials have been applied to the gas detection field, such as Zhou [22], [23] et al. studied CO gas sensors based on SnO<sub>2</sub> nanomaterials with different dopant, and high sensitivity CO gas sensor was developed; Lin [24] et al. investigated the H<sub>2</sub> sensing properties of Pt-loaded SnO<sub>2</sub> hollow microspheres, and hydrogen sensor at room temperature is obtained with fast response properties. However, only one key characteristic gas is studied in these studies.

Actually, the semiconductor gas sensor is sensitive to most of the fault gases dissolved in transformer oil. This phenomenon is called cross-sensitivity. In practical application of DGA, the gases are mixtures. Hence, the selectivity and quantitative accuracy problem of semiconductor gas sensor is still to be solved for the detection of mixed gas. To address this problem, Fan [15], [25] et al. applied the SnO<sub>2</sub> sensor as a chromatographic detector which is used for DGA, promising experimental results are obtained. The above studies mainly concentrate on low concentration gases detection, i.e., H<sub>2</sub> < 100ppm. For practical engineering application, there may be higher concentrations, e.g., hydrocarbons may rise up to 1000ppm (0.1%) due to partial discharge faults.

To promote the performance of SnO<sub>2</sub> detector further, in this work, the detection characteristics of nanometer tin oxide sensor are studied; then, a quantitative mathematical model on basis of exponent-logarithmic model is constructed. Further, the preparation process, test steps of the developed nanometer tin oxide sensor is introduced. To promote the detection limit of SnO<sub>2</sub> detector, the chromatographic signal noise reduction algorithms based on different wavelet are studied. The experiment results show that the gas chromatography detection technology of nanometer tin oxide can realize detection of the fault characteristic gases, i.e., H<sub>2</sub>, CH<sub>4</sub>, CO, C<sub>2</sub>H<sub>4</sub>, C<sub>2</sub>H<sub>6</sub>, and C<sub>2</sub>H<sub>2</sub> without cross-sensitivity. Based on the mathematical model as well as the noise reduction algorithm constructed in this paper, wide measurement range as well as high precision can be achieved simultaneously. Meanwhile, only air is needed to be carrier gas, the overall cost of the system is reduced, which has important popularization value.

## II. DETECTOR FABRICATION AND QUANTIFICATION MODEL

Given that the SnO<sub>2</sub> gas sensors is used as an chromatographic detector in this paper, namely, H<sub>2</sub>, CO, CH<sub>4</sub>, C<sub>2</sub>H<sub>4</sub>, C<sub>2</sub>H<sub>6</sub>, C<sub>2</sub>H<sub>2</sub> are separated though chromatographic column and detected simultaneously. Hence, considering the sensitivity equilibrium for all gases, none specific dopant is added and pure SnO<sub>2</sub> is adopted. In this work, the tin oxide nano-materials are prepared by electrospinning [26]. To verify the nanostructures of the samples, XRD, TEM and HRTEM are performed; the corresponding images are shown in Figs.1 (a)-(c). The diffraction peaks match well with the standard data of rutile structured SnO<sub>2</sub> crystal (JCPDS file no.41-1445). It is notably that the diameter of SnO<sub>2</sub> fiber is about 100~200nm and the lattice distance on (110) surface is 0.334nm. The nanometer tin oxide materials are fully grinded

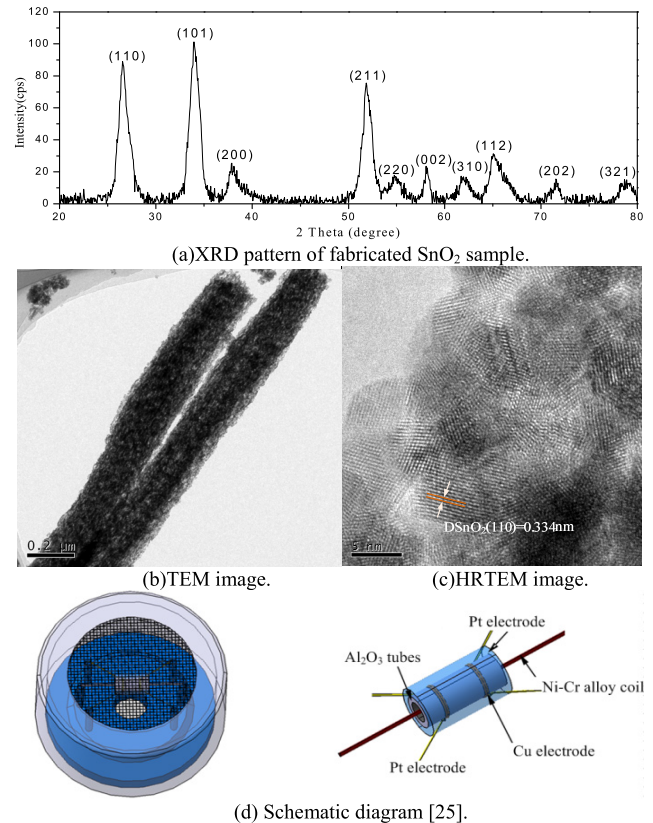


**FIGURE 1.** SnO<sub>2</sub> fiber characterization images and schematic diagram of Nano-SnO<sub>2</sub> sensor.

in the agate mortar, adding the appropriate anhydrous ethanol and deionized water to make the slurry, brushing on the alumina ceramic tube with electrode leads which are welded on the surface of the tube.

The package with the sensor is installed in a gas chromatographic instrument developed in this paper. The schematic diagram of Nano-SnO<sub>2</sub> sensor is shown in Fig.1. When acting as a chromatographic detector, the characteristic gases extracted from transformer oil is brought into chromatographic column (CC) by carrier gas (99.999% synthetic air), and the temperature of CC as well as the sensor package are set to 60°C. Due to the difference of the distribution coefficients between the gas and the CC [28], the characteristic gases are separated in sequence. The separated six gases flow into the sensor package as shown in Fig.2, and then flow out after a sensitive reaction occurs on the surface of the detector. When the combustible gases react with the oxygen adsorbed on the surface of the sensor, the electrons are released into the depletion layer of the sensing material, hence leading to augment of the conductivity [16], and the output voltage becomes larger. Hence, the output voltage signal is proportional to the conductance of the nanometer tin oxide detector.

According to the theoretical analysis, the detector is mostly used to detect reductive gases; it is not sensitive to other gases such as nitrogen, carbon oxide, et al. For the analysis of dissolved gas in oil, gas detection is performed

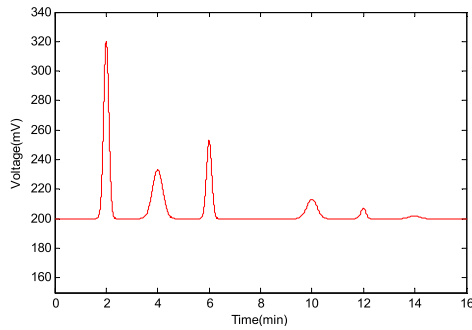


FIGURE 2. Simulated chromatogram without noise.

after separation, which avoids the cross sensitivity of traditional detection method. In terms of quantitative model, the mathematical model proposed in [15] is mainly applied for hydrogen < 100ppm, as well as hydrocarbons < 300ppm. However, hydrogen may rise up to 0.1% due to partial discharge faults. Hence, the measurement range should be further improved. Considering that the inverse equation of Eq.(15) in Ref. [15] contains the Lambert W function [27], which is complicated in practical application. Meanwhile, the fault feature gases are limited within a certain concentration interval (<1000ppm usually), hence the relation between conductance and gas concentration can be approximated well by exponent-logarithmic model, which is:

$$G = a_1 \exp(a_2 \ln(C)) + a_3 \quad (1)$$

In Eq.(6),  $a_1$ ,  $a_2$  and  $a_3$  are the parameters determined by different gases. When none combustible gases exist on the surface of the sensor, electrons transferred to adsorbed oxygen, the number of electrons on the semiconductor surface decreases, leading to increment of the gas sensor's resistivity. On the other hand, when combustible gases contact with the sensor, reactions between the tested gas and oxygen ions release electrons, leading to increment of the gas sensor's conductivity. Correspondingly, the change amount of conductivity is proportional to the concentration of combustible gas (CG), the higher concentration of the CG, the greater change of the conductivity.

Generally, peak height or peak area is used as the quantitative method of gas chromatography, according to the linear relationship between peak height (or peak area) and gas concentration. Based on which, the unknown gas concentration is determined by the look-up-table method. According to Eq.(1) which is not linear, shows that the conductivity of the semiconductor tin oxide sensor is exponent-logarithmic related to the gas concentration change, and there would be large error if using the traditional peak height or peak area linear fitting method. For semiconductor tin oxide sensor, the change of peak height or peak area is the change of conductance. In practical application, to determine the three parameters:  $a_1$ ,  $a_2$ ,  $a_3$ , the sensor should be calibrated. When the gas concentration is  $C_1$  which corresponds to the conductance of the sensor is  $G_1$ , the gas concentration is  $C_2$  which corresponds to the conductance of the sensor is  $G_2$ ,

hence, for  $n$  different concentrations of standard gases, the corresponding concentration and conductance of vectors can be written as:  $G = (G_1, G_2 \dots G_n)$ ,  $C = (C_1, C_2 \dots C_n)$ . Substitute the two vectors into Eq.(1), an equation group can be obtained:

$$\begin{cases} G_1 = a_1 \exp(a_2 \ln(C_1)) + a_3 \\ G_2 = a_1 \exp(a_2 \ln(C_2)) + a_3 \\ \vdots \\ G_n = a_1 \exp(a_2 \ln(C_n)) + a_3 \end{cases} \quad (2)$$

By using least square method, the nonlinear equation group can be solved, and the value of the parameters  $a_1$ ,  $a_2$ ,  $a_3$  can be determined. On this basis, the unknown concentration  $C$  can be obtained according to the measured conductance change  $G$ . For DGA application of this paper, the sensor is calibrated by using five sets of standard gases to determine the model parameters.

### III. EXPERIMENT

Due to the cross sensitivity of the semiconductor sensor, the characteristic gases must be separated before detection. The separation of gas mixtures using GC is based on the fact that the adsorption coefficient is different between gases and stationary phases [28], and the separation is realized by the chromatographic column. There are two factors, namely, amount of sampling gas and separation degree which affect performance of the GC system directly. The consistency of former has great influence on the measurement repeatability, while the later is evaluated by the retention time (RT) differences of each component.

In order to validate the correctness of the proposed model on the developed sensor, a chromatography instrument is developed. The sensor is integrated with the temperature control as well as data acquisition module [25], the latter convert resistance of the sensor into the voltage. The collected data is sent to the special chromatographic software. When the test process is performed, the package of the sensor and CC are set to 60°C. Prepare the standard gas from high to low concentration as different samples. After the temperature of CC stabilized at 60±0.1°C, as well as the fluctuation of baseline is less than 0.5mV/min, the prepared samples are then transferred to the sampling loop, and then the chromatogram is sampled and recorded by utilizing the data acquisition unit. There may exist trace concentration of propane in the mixture gases extracted from the oil. Its concentration is so low that there may be only a slight fluctuation of the baseline. Considering the baseline stabilization, after the last peak, i.e., C<sub>2</sub>H<sub>2</sub>, flows out from the column, another 15min are reserved before next experiment so that propane can flow out as one single peak in this period.

#### A. SIGNAL PROCESSING

To separate small peaks from the chromatographic signal (for detection of incipient transformer faults), signal denoising is crucial to promote signal-noise-ratio (SNR) [28]. In terms

of chromatographic signal denoising, discrete wavelet theory (DWT) is used largely, and the detail of which can refer to [29], [30]. Actually, the denoising is based on the fact that the DWT decomposition coefficients of the chromatogram are restricted to approximation coefficients, the signal components are large, while the amplitude of noises' coefficients are small and distributed in detailed coefficients [29], [30]. Hence, though thresholding the small coefficients, the denoising of the signal can be realized. When the DWT is performed for denoising, many parameters are needed to be determined [31].

In order to reconstruct the signal perfectly after wavelet denoising, orthogonal mother wavelet should be chosen [31], e.g., Coiflet, Symlet and Daubechies, et al. In terms of the second parameter, namely, the decomposition levels should be determined carefully such that the noise components can be eliminated efficiently. The wavelet and decomposition level  $k$  can be determined by the method proposed in [32] in practical application.

The third parameter is threshold value, which is critical in DWT. A small threshold value is ineffective to eliminate noises, while the useful signal components would be lost if a large value of threshold is selected. Presently, the most widely used methods for threshold estimation [31], [33] are 'rigrsure', 'heursure', 'sqrtwolog', and 'minimaxi', respectively. The 'sqrtwolog' method determines the threshold by the length of the signal, but content of the signal is not taken into account. 'minimaxi' is evaluated by minimizing the maximum risk of estimation error, and it is a fixed threshold method. In terms of 'rigrsure' method, a threshold value is determined by minimizing the Steins unbiased risk estimation (SURE). For 'heursure' method, one of 'sqrtwolog' or 'rigrsure' method is selected after SNR estimation. In fact, different methods yield to different results [34].

The threshold function is the fourth parameter, it determines the way to for wavelet coefficients treatment based on the threshold value. Commonly, there are two types of threshold functions, namely soft and hard functions. For two types of threshold functions, the coefficients which are smaller than the thresholds are set to zeros. The other coefficients are shrunk by using soft threshold function. However, in hard threshold function they remain unchanged. Generally, larger SNR value can be obtained by using hard threshold function; however, there are discontinuities in the reconstructed signal. Hence, soft threshold function is applied in this paper.

In this paper, the genetic threshold wavelet algorithm (GTWA) [25] is adopted for signal denoising. To determine optimal parameters for weak signal extraction, the noisy chromatogram is simulated using the following expression [28]:

$$f(t) = \sum_{i=1}^N \frac{A_i}{\sigma \sqrt{2\pi}} \exp[-\frac{1}{2}(\frac{t-t_{Ri}}{\sigma})^2], \quad i = 1, 2, \dots, N. \quad (3)$$

where  $A_i$  is the area of  $i^{\text{th}}$  peak,  $t_{Ri}$  is the retention time of the  $i^{\text{th}}$  peak. Because the characteristic gas dissolved in transformer oil have six components, i.e.,  $H_2$ ,  $CO$ ,  $CH_4$ ,

TABLE 1. Parameters of simulated chromatogram.

Component	$H_2$	$CO$	$CH_4$	$C_2H_4$	$C_2H_6$	$C_2H_2$
Peak area	30	10	20	5	3	1
Peak height	120	166	53	13	7	2
Retention time	2	4	6	10	12	14
Standard deviation	0.1	0.12	0.15	0.15	0.17	0.2

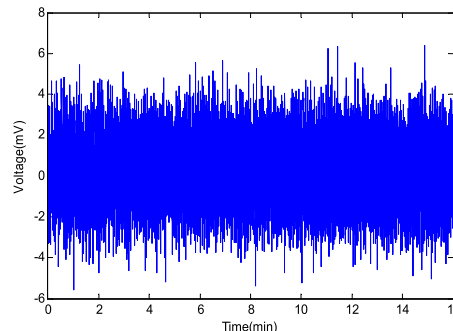


FIGURE 3. Simulated noise.

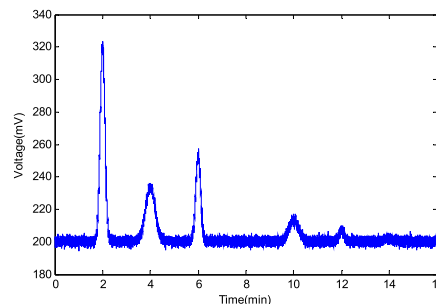


FIGURE 4. Simulated chromatogram with noise addition.

$CH_4$ ,  $C_2H_6$ , and  $C_2H_2$ , six chromatographic peaks have been simulated and produced. Similar to the actual application, all chromatographic peaks are concentrated in 15 minutes, the baseline is set to 200mV. The detailed parameters of the simulation are shown in Table 1, and the corresponding simulated chromatogram is shown in Fig.2.

In the actual engineering application, due to the noises in chromatogram, random noises are added to the chromatogram in the simulation. The additive noises are simulated as follows:

$$s(t) = f(t) + \frac{0.5 - b * randn}{a} \quad (4)$$

where  $s(t)$  is the produced noisy chromatogram curve;  $a$ ,  $b$  are the constants to control SNR,  $randn$  is the Gaussian white noise generated using MATLAB, when  $a = 2$ ,  $b = 3$ , the simulated noise and corresponding chromatogram are shown in Figs.3~4, respectively.

It can be seen from Fig.3 that the positive maximum value of noise amplitude is 6.4017mV, and the negative maximum value is -5.5696mV. In terms of the region 13~15min where acetylene locates, the noises are 3.3908mV and -4.2067mV, respectively. However, the peak height of acetylene is only setup to 2mV, which is drowned out by noise pollution. As a result, Fig.4 is the simulated chromatogram which can be

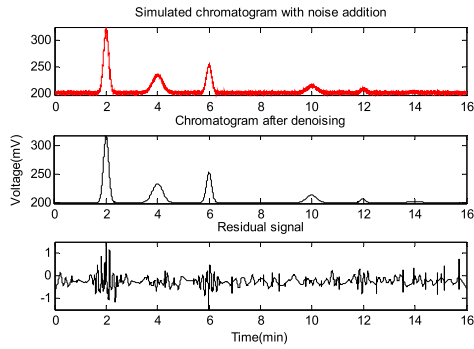


FIGURE 5. Validity of signal denosing algorithm.

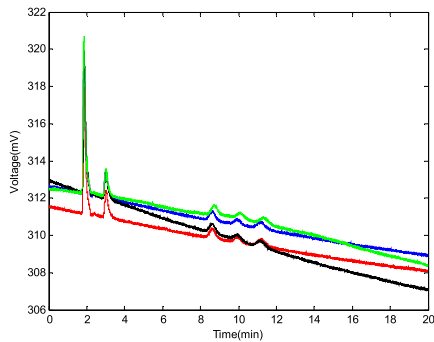


FIGURE 6. Actual measured chromatogram (dissolved gas in oil) with noise.

used to verify the validity of denosing algorithm. On basis of this chromatogram, the signal extraction ability of the GTWA can be maximized, and the optimal parameters can be obtained, which are as follows: decomposition level  $k = 6$ , sym4, soft threshold function, the results are shown in Fig.5.

As shown in Fig.5, the weak acetylene peak can be extracted from the noisy chromatogram; the peak height is 1.99mV after denosing, which almost keep the same height (2mV) with original signal and indicates validity of the proposed signal denosing algorithm. After the optimal wavelet parameters for denoising are determined by the simulated chromatogram, the signal extraction ability of the algorithm on the actual measured chromatogram is needed to be verified. Unlike the simulated chromatogram, the actual chromatogram is often with a baseline drift. Moreover, for most of the transformer oil, the gas concentration of each component (especially acetylene) is low; hence the corresponding peak is weak, which is usually submerged by noises.

The actual measured chromatographic signals of four developed detectors in this work are shown in Fig.6. As shown in Fig.6, the baseline of the chromatographic SnO<sub>2</sub> detector is somewhat oblique. The reason is that there is “baseline stabilization time” for any chromatographic detectors, including the SnO<sub>2</sub> chromatographic detector. It is notable that the baseline drifts are in the range of 0.14~0.3mV/min, within which the measurement accuracy is not affected.

The corresponding denoised chromatogram using common threshold wavelet algorithm (CTWA) with sqtwolog rule and

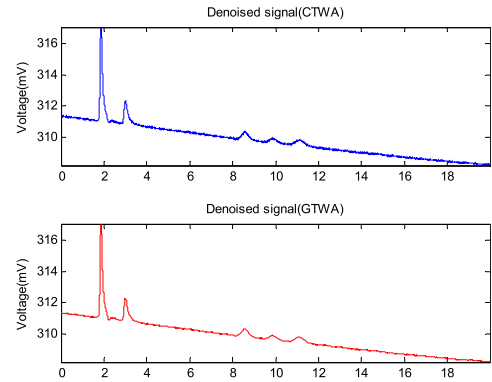


FIGURE 7. Sqtwolog rule of wavelet threshold denoising result vs. genetic wavelet algorithm using soft threshold function.

TABLE 2. Comparison of different denoising algorithm.

Method	Soft threshold function		Hard threshold function	
	Noise(mV)	SNR	Noise(mV)	SNR
CTWA	0.12	2.5	0.13	2.3
GTWA	0.04	7.5	0.07	4.3

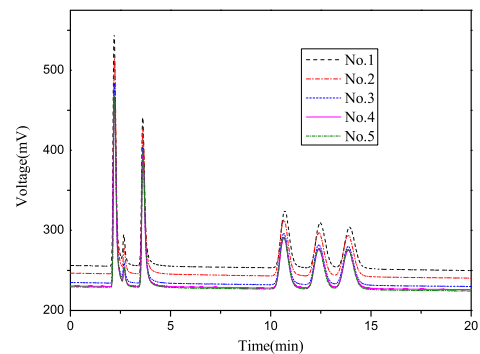


FIGURE 8. Repeatability tests using the same concentration.

TABLE 3. Standard gas concentration for calibration (ppm).

	H <sub>2</sub>	CO	CH <sub>4</sub>	C <sub>2</sub> H <sub>4</sub>	C <sub>2</sub> H <sub>6</sub>	C <sub>3</sub> H <sub>2</sub>
1	3.37	14.21	1.33	3.98	1.99	1.22
2	4.475	28.47	4.215	4.945	5.87	5.385
3	14.125	69.985	10.81	11.48	13.725	11.28
4	114.37	434.7	63.39	59.29	49.82	58.72
5	480.63	1835.98	530.61	578.1	576.51	592.2

GTWA are shown in Fig.7. As seen from Fig.7, the GTWA has better denoising effect. Compared with CTWA method, the obtained chromatogram using GTWA is smoother, indicating higher SNR. However, there still exist noises after using the ‘sqtwolog’ rule of CTWA, especially when the gas concentration is low and the noise is large. With the increment of gas concentration, the peak height becomes larger while the noise is unchanged, SNR becomes higher, the differences between the CTWA and the GTWA decreases, hence GTWA is especially suitable for the extraction of the weak signals in the chromatograms with large noises and low gas concentration.

Take acetylene for example, after wavelet denoising, the SNR with different wavelet algorithm are shown in Table 2, from which it can be seen that the SNR with

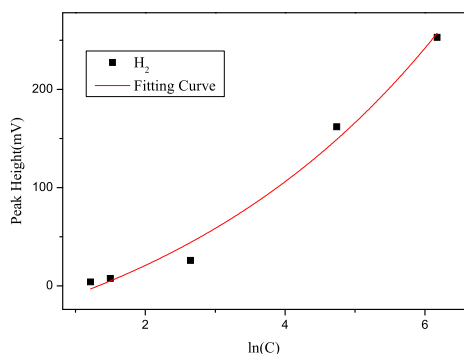


FIGURE 9. Correlation of peak height versus logarithm of concentration (H<sub>2</sub>).

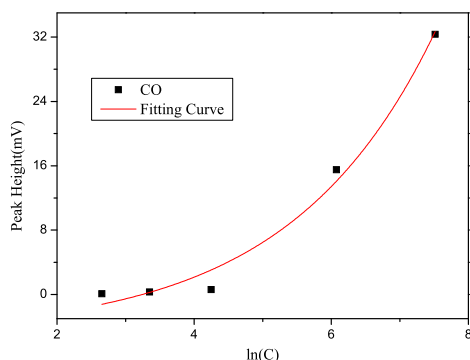


FIGURE 10. Correlation of peak height versus logarithm of concentration (CO).

GTWA is increased more than three times. Hence, the minimum detection limit of acetylene will be promoted the corresponding multiples when the sensor’s sensitivity remains unchanged, thus providing a good foundation for discovering the early faults of power transformer.

**B. QUANTITATIVE RESULTS**

For chromatographic detector, quantitative repeatability is important for performance evaluation. The stability of peak height or peak area is usually used to evaluate the repeatability. According to reference [35], the relative standard deviation (RSD) can be calculated from Eq.(5) for the sequence

$$G = (G_1, G_2 \dots G_n):$$

$$RSD = \frac{\sqrt{\sum_{i=1}^n (G_i - \bar{G})^2}}{(n - 1)\bar{G}} \times 100\% \tag{5}$$

In Eq.(5), n indicates the number of detection records;  $\bar{G}$  represents the average peak height;  $G_i$  represents the conductance of the  $i^{th}$  records; i is the numerical record of testing number. In order to test the repeatability, the standard gas is analyzed using the developed instrument, the standard gas concentrations are as follows: H<sub>2</sub> is 480.63  $\mu$ L/L, CO is 1835.98  $\mu$ L/L, CH<sub>4</sub> and 530.61  $\mu$ L/L, C<sub>2</sub>H<sub>4</sub> is 578.1  $\mu$ L/L, C<sub>2</sub>H<sub>6</sub> is 576.51  $\mu$ L/L, C<sub>2</sub>H<sub>2</sub> is 592.2  $\mu$ L/L. Repeat the test five times, the peak height of the chromatogram are recorded, as shown in Fig.8. The RSD values of the six gases tested are: H<sub>2</sub>:8.5%, CO:7.5%, CH<sub>4</sub>:4.7%, C<sub>2</sub>H<sub>4</sub>:5.6%, C<sub>2</sub>H<sub>6</sub>:6.2%, C<sub>2</sub>H<sub>2</sub>:3.4%, meeting the requirements that less than 10% in IEC 60599-2015.

In order to examine performance of the detector, and verify validity of the quantitative algorithm proposed in this paper, based on Eq.(1), the detector’s response to six characteristic gases at different concentrations shown in Table 3 were carefully tested in this work, and the standard gases are stored in gas cylinders and produced by commercial gas company. The correlations of the logarithm of the concentration versus the peak height were obtained, as shown from Figs.9~12.

From Figs.9~12, the fitting curves show well coincidence for the proposed model of which corresponding regression equations (RE) are listed in Table 4, as well as correlation coefficient, linear range, and detection limits for six characteristic gases. As shown in the Table 4, the responses of the detector agrees well with the established model with a correlation coefficient >0.9 for all gases (larger than 0.99 for four hydrocarbons). Based on the REs, the detection limits (DL) were calculated by using double amplitude of noise (i.e., obtained results in Table 2) in the REs. The purpose of the detector and the corresponding GC system is designed for relative large concentration measurement, the DL is about 1 ppm to hydrocarbons, e.g., 1ppm (v/v) for acetylene.

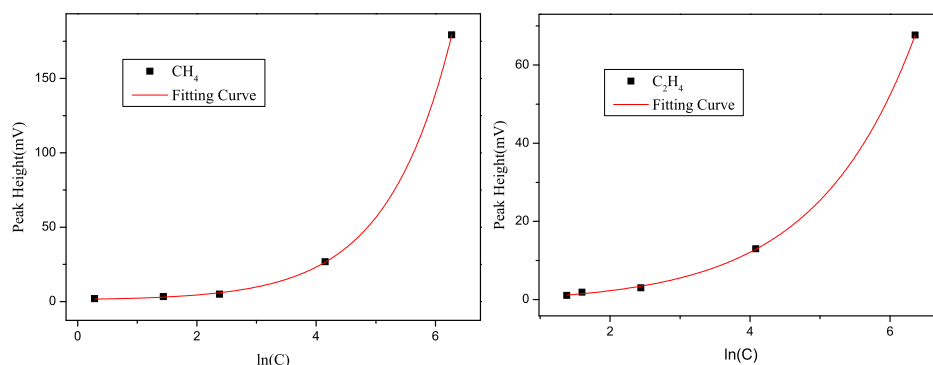


FIGURE 11. Correlation of peak height versus logarithm of concentration (CH<sub>4</sub> \ C<sub>2</sub>H<sub>4</sub>).

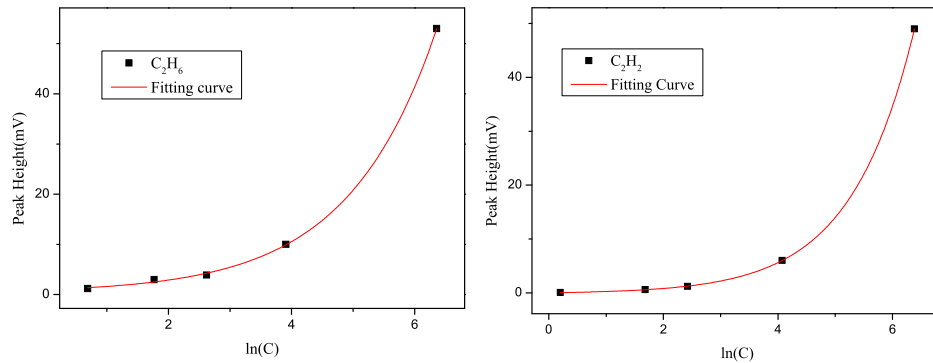


FIGURE 12. Correlation of peak height versus logarithm of concentration ( $C_2H_6/C_2H_2$ ).

TABLE 4. Parameters of fitting curve and performance of the detector.

Compounds	Regression equation	$R^2$	Tested range (ppm)	Detection limits (ppm)
$H_2$	$G = 89.88\exp(0.23\ln(C)) - 117.37$	0.9769	3.37~480.63	3.19
CO	$G = 1.08\exp(0.47\ln(C)) - 4.01$	0.9756	14.21~1835.98	8.98
$CH_4$	$G = 0.58\exp(0.91\ln(C)) - 0.6$	0.9999	1.33~530.61	1.08
$C_2H_4$	$G = 0.78\exp(0.7\ln(C)) - 0.89$	0.9997	3.98~578.1	1.25
$C_2H_6$	$G = 0.37\exp(0.63\ln(C)) - 0.3$	0.9998	1.99~576.51	1.04
$C_2H_2$	$G = 0.16\exp(0.9\ln(C)) - 0.14$	1	1.22~592.2	1.0

Usually, regarding DGA for power transformer, FID + TCD is the frequent used detector in laboratory, whose results can be taken as references for other sensors, e.g.,  $SnO_2$  sensor, SOFC, or PSS. In order to compare the results with FIDs, experiments are performed to test the same sample gas using the developed detector. Compared with FID + TCD, all of the relative errors are less than 10%, which indicates that similar measurement precision can be achieved by utilizing the chromatographic detector of this work and proposed quantitative algorithm. Notably, only air is needed to be the carrier gas, based on which the hardware cost of the GC is reduced. Unlike FID + TCD, no hydrogen which is flammable gas is needed, hence the structure of the system is simplified and the security can be improved. It is worth mentioning that the degassing process of transformer oil is not considered in the calculation process, in the practical application of engineering, gas extraction methods, e.g., shaking technique [36], or vacuum degasification [37] are commonly used techniques, in which the degassing rate and oil temperature should be considered, and the gas-in-gas value should be corrected to obtain the final gas-in-oil results.

#### IV. CONCLUSION

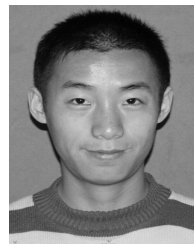
- (1) The gas sensing mechanism for measuring six-component gases dissolved in transformer oil by nanometer tin oxide semiconductor chromatographic detector is expounded. A GC system based on one-dimensional nanometer tin oxide fiber material is developed.

- (2) To extract small peaks from the chromatographic signal, GTWA method is adopted for chromatogram denoising. The exponent-logarithmic model between the conductance of  $SnO_2$  sensor and combustible gas concentration has been proposed, based on which the repeatability and accuracy are tested, and the validity of the proposed model was validated.
- (3) Combined gas chromatographic system with nanometer tin oxide detector, the cross-sensitivity problem of mixture detection can be effectively solved. Meanwhile, the exponent-logarithmic quantitative model proposed in this paper is more suitable than the traditional linear fitting method on basis of chromatographic peak height or peak area. Only air is needed to be carrier gas, which reduces the cost and complexity of the hardware system, has important engineering application value.

#### REFERENCES

- [1] H. Faria, Jr., J. G. S. Costa, and J. L. M. Olivas, "A review of monitoring methods for predictive maintenance of electric power transformers based on dissolved gas analysis," *Renew. Sustain Energy Rev.*, vol. 46, pp. 201–209, Jun. 2015.
- [2] Y.-C. Huang and H.-C. Sun, "Dissolved gas analysis of mineral oil for power transformer fault diagnosis using fuzzy logic," *IEEE Trans. Dielectr. Electr. Insul.*, vol. 20, no. 3, pp. 974–981, Jun. 2013.
- [3] J. Fan, F. Wang, Q. Q. Sun, F. Bin, F. Liang, and X. Xiao, "Hybrid RVM-ANFIS algorithm for transformer fault diagnosis," *IET Gener., Transmiss. Distrib.*, vol. 11, no. 14, pp. 3637–3643, 2017.
- [4] F. C. Sica, F. G. Guimarães, R. de Oliveira Duarte, and A. J. R. Reis, "A cognitive system for fault prognosis in power transformers," *Electr. Power Syst. Res.*, vol. 127, pp. 109–117, Oct. 2015.

- [5] S. A. Khan, M. D. Equbal, and T. Islam, "A comprehensive comparative study of DGA based transformer fault diagnosis using fuzzy logic and ANFIS models," *IEEE Trans. Dielectr. Electr. Insul.*, vol. 22, no. 1, pp. 590–596, Feb. 2015.
- [6] J. Jiang, M. Zhao, G.-M. Ma, H.-T. Song, C.-R. Li, X. Han, and C. Zhang, "TDLAS-based detection of dissolved methane in power transformer oil and field application," *IEEE Sensors J.*, vol. 18, pp. 2318–2325, Mar. 2018.
- [7] D. Jiejie, S. Hui, and S. Gehao, "Dissolved gas analysis of insulating oil for power transformer fault diagnosis with deep belief network," *IEEE Trans. Dielectr. Electr. Insul.*, vol. 24, no. 5, pp. 2828–2835, Oct. 2017.
- [8] R. Naresh, V. Sharma, and M. Vashisth, "An integrated neural fuzzy approach for fault diagnosis of transformers," *IEEE Trans. Power Del.*, vol. 23, no. 4, pp. 2017–2024, Oct. 2008.
- [9] Z. Mao and J. Wen, "Detection of dissolved gas in oil-insulated electrical apparatus by photoacoustic spectroscopy," *IEEE Trans. Dielectr. Electr. Insul.*, vol. 31, no. 4, pp. 7–14, Apr. 2015.
- [10] Q. Zhou, W. Chen, L. Xu, and S. Peng, "Hydrothermal synthesis of various hierarchical ZnO nanostructures and their methane sensing properties," *Sensors*, vol. 13, no. 5, pp. 6171–6182, 2013.
- [11] A. I. Uddin, U. Yaqoob, and G.-S. Chung, "Dissolved hydrogen gas analysis in transformer oil using Pd catalyst decorated on ZnO nanorod array," *Sens. Actuators B, Chem.*, vol. 226, pp. 90–95, Jan. 2016.
- [12] J. Lu, X. Zhang, X. Wu, Z. Dai, and J. Zhang, "A Ni-doped carbon nanotube sensor for detecting oil-dissolved gases in transformers," *Sensors*, vol. 15, no. 6, pp. 13522–13532, 2015.
- [13] M. Fisser, R. A. Badcock, P. D. Teal, and A. Hunze, "Optimizing the sensitivity of palladium based hydrogen sensors," *Sens. Actuators B, Chem.*, vol. 259, pp. 10–19, Apr. 2018.
- [14] B. Jang, M. Kim, J. Baek, W. Kim, and W. Lee, "Highly sensitive hydrogen sensors: Pd-coated Si nanowire arrays for detection of dissolved hydrogen in oil," *Sens. Actuator B, Chem.*, vol. 273, pp. 809–814, Nov. 2018.
- [15] J. Fan, F. Wang, Q. Sun, F. Bin, H. Ye, and Y. Liu, "An online monitoring system for oil immersed power transformer based on SnO<sub>2</sub> GC detector with a new quantification approach," *IEEE Sensors J.*, vol. 17, no. 20, pp. 6662–6671, Oct. 2017.
- [16] F. Wang, J. Fan, Q. Sun, Q. Jiang, S. Chen, and W. Zhou, "Adsorption mechanism of Cu-doped SnO<sub>2</sub> (110) surface toward H<sub>2</sub> dissolved in power transformer," *J. Nanomater.*, vol. 2016, Nov. 2016, Art. no. 3087491.
- [17] J. Ding, X. Li, J. Cao, L. Sheng, L. Yin, and X. Xu, "New sensor for gases dissolved in transformer oil based on solid oxide fuel cell," *Sens. Actuators B, Chem.*, vol. 202, pp. 232–239, Oct. 2014.
- [18] J. Fan, F. Wang, Q. Sun, F. Bin, J. Ding, and H. Ye, "SOFC detector for portable gas chromatography: High-sensitivity detection of dissolved gases in transformer oil," *IEEE Trans. Dielectr. Electr. Insul.*, vol. 24, no. 5, pp. 2854–2863, Oct. 2018.
- [19] F. Rastrello, P. Placidi, A. Scorzoni, E. Cozzani, M. Messina, I. Elmi, S. Zampolli, and G. C. Cardinali, "Thermal conductivity detector for gas chromatography: Very wide gain range acquisition system and experimental measurements," *IEEE Trans. Instrum. Meas.*, vol. 62, no. 5, pp. 974–981, May 2013.
- [20] J. Jalbert and R. Gilbert, "Decomposition of transformer oils: A new approach for the determination of dissolved gases," *IEEE Trans. Power Del.*, vol. 20, no. 2, pp. 754–760, Feb. 1997.
- [21] Z. Jiang, R. Zhao, B. Sun, G. Nie, H. Ji, J. Lei, and C. Wang, "Highly sensitive acetone sensor based on Eu-doped SnO<sub>2</sub> electrospun nanofibers," *Ceramics Int.*, vol. 42, no. 14, pp. 15881–15888, 2016.
- [22] Q. Zhou, L. Xu, A. Umar, W. Chen, and R. Kumar, "Pt nanoparticles decorated SnO<sub>2</sub> nanoneedles for efficient CO gas sensing applications," *Sens. Actuators B, Chem.*, vol. 256, pp. 656–664, Mar. 2018.
- [23] Q. Zhou, W. Chen, L. Xua, R. Kumar, Y. Gui, Z. Zhao, C. Tang, and S. Zhu, "Highly sensitive carbon monoxide (CO) gas sensors based on Ni and Zn doped SnO<sub>2</sub> nanomaterials," *Ceramics Int.*, vol. 44, pp. 4392–4399, Mar. 2018.
- [24] B. Lin, F. Jia, B. Lv, Z. Qin, P. Liu, and Y. Chen, "Facile synthesis and remarkable hydrogen sensing performance of Pt-loaded SnO<sub>2</sub> hollow microspheres," *Mater. Res. Bull.*, vol. 106, pp. 403–408, Oct. 2018.
- [25] J. Fan, F. Wang, Q. Sun, H. Ye, and Q. Jiang, "Application of polycrystalline SnO<sub>2</sub> sensor chromatographic system to detect dissolved gases in transformer oil," *Sens. Actuator B, Chem.*, vol. 267, pp. 636–646, Aug. 2018.
- [26] F. Li, T. Zhang, X. Gao, R. Wang, and B. Li, "Coaxial electrospinning heterojunction SnO<sub>2</sub>/Au-doped In<sub>2</sub>O<sub>3</sub> core-shell nanofibers for acetone gas sensor," *Sens. Actuator B, Chem.*, vol. 252, pp. 822–830, Nov. 2017.
- [27] C. Schultealbert, T. Baur, A. Schütze, S. Böttcher, and T. Sauerwald, "A novel approach towards calibrated measurement of trace gases using metal oxide semiconductor sensors," *Sens. Actuators B, Chem.*, vol. 239, pp. 390–396, Feb. 2017.
- [28] H. M. McNair and J. M. Miller, *Basic Gas Chromatography*, 2nd ed. Hoboken, NJ, USA: Wiley, 2009, pp. 140–144.
- [29] K. K. Shukla and A. K. Tiwari, *Efficient Algorithms for Discrete Wavelet Transform*. London, U.K.: Springer, 2013.
- [30] M. Jansen, *Noise Reduction by Wavelet Thresholding*. New York, NY, USA: Springer, 2001.
- [31] P. K. Jain and A. K. Tiwari, "An adaptive thresholding method for the wavelet based denoising of phonocardiogram signal," *Biomed. Signal Process. Control*, vol. 38, pp. 388–399, Sep. 2017.
- [32] M. Srivastava, C. L. Anderson, and J. H. Freed, "A new wavelet denoising method for selecting decomposition levels and noise thresholds," *IEEE Access*, vol. 4, pp. 3862–3877, 2016.
- [33] M. S. Sadooghi and S. E. Khadem, "A new performance evaluation scheme for jet engine vibration signal denoising," *Mech. Syst. Signal Process.*, vols. 76–77, pp. 201–212, Aug. 2016.
- [34] P. Nguyen and J.-M. Kim, "Adaptive ECG denoising using genetic algorithm-based thresholding and ensemble empirical mode decomposition," *Inf. Sci.*, vol. 373, pp. 499–511, Oct. 2016.
- [35] H. Meng, W. Yang, X. Yan, Y. Zhang, L. Feng, and Y. Guan, "A highly sensitive and fast responsive semiconductor metal oxide detector based on In<sub>2</sub>O<sub>3</sub> nanoparticle film for portable gas chromatograph," *Sens. Actuator B, Chem.*, vol. 216, pp. 511–517, Sep. 2015.
- [36] G. M. C. Vinicius, A. L. H. Costa, and M. L. L. Paredes, "Development and evaluation of a new DGA diagnostic method based on thermodynamics fundamentals," *IEEE Trans. Dielectr. Electr. Insul.*, vol. 22, no. 2, pp. 888–894, Apr. 2015.
- [37] A. Zhao, X. Tang, J. Liu, and Z. Zhang, "The on-site DGA detecting and analysis system based on the Fourier transform infrared instrument," in *Proc. IEEE Int. Instrum. Meas. Technol. Conf. (IMTC)*, May 2014, pp. 1036–1040.



**JINGMIN FAN** received the B.Eng. and M.Eng. degrees in electronic science and technology from Central South University, Changsha, China, in 2007 and 2010, respectively. He received the Ph.D. degree in electrical engineering from Hunan University, Changsha, China, in 2018. He is currently an Associate Professor with the Guangdong University of Technology. His research interests include intelligent algorithm and state evaluation of power equipment.



**ZHE LIU** received the B.Sc. degree in electrical engineering from Hunan Institute of Engineering, Xiangtan, China, in 2016. He is currently pursuing the M.Sc. degree with the School of Automation, Guangdong University of Technology, Guangdong, China. His research interests include state evaluation of power equipment, microgrids, and intelligent control.

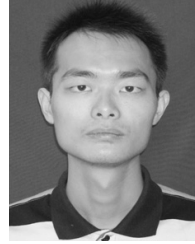


**ANBO MENG** received the B.Eng. and M.Eng. degrees in water conservancy and hydropower engineering from North China University of Water Resources and Electric Power, Zhengzhou, China, in 1995 and 2001, respectively. He received the Ph.D. degree in automation from Université Paul Verlaine-Metz, Metz, France, in 2008. He is currently a Professor in electrical engineering with the Guangdong University of Technology, Guangzhou, China. His research interests include intelligent algorithm and state evaluation of power equipment.





**HAO YIN** received the B.Eng. and M.Eng. degrees in water conservancy and Hydropower Engineering from North China University of Water Resources and Electric Power, Zhengzhou, China, in 1996 and 1999, respectively. She is currently an Associate Professor in electrical engineering with the Guangdong University of Technology, Guangzhou, China. Her research interest includes state evaluation of power equipment.



**FENG BIN** received the B.Sc. and M.Sc. degrees from School of Physical and electronic science, Changsha University of Science & Technology, Changsha, China, in 2012 and 2015, respectively. He is currently pursuing the Ph.D. degree with the College of Electrical and Information Engineering, Hunan University, Changsha, China. His research interests include state evaluation of power equipment, partial discharge detection, and signal processing.



**QIUQIN SUN** received the B.Eng. degree in electrical engineering from Chongqing University, Chongqing, China, in 2006 and the Ph.D. degree in electrical engineering from Shandong University, Jinan, China, in 2012. He is currently an Assistant Professor with Hunan University, Changsha, China.



**QINJI JIANG** received the B.Eng. and M.Eng. degrees in electrical engineering from Hunan University, Changsha, China, in 2013 and 2016, respectively. He is currently a Junior Engineer with the State Grid Hunan Maintenance Company, Changsha, China. His research interest includes the electric power planning.

...